Biosensors and Bioelectronics 142 (2019) 111510

Contents lists available at ScienceDirect

Biosensors and Bioelectronics

journal homepage: www.elsevier.com/locate/bios

DNA synergistic enzyme-mediated cascade reaction for homogeneous electrochemical bioassay

Yaxing Zhang[a], Xiyue Cao[a], Ruixue Deng[a], Qingyun Liu[b], Jianfei Xia[a,*], Zonghua Wang[a]

[a] College of Chemistry and Chemical Engineering, Shandong Sino-Japanese Center for Collaborative Research of Carbon Nanomaterials, Collaborative Innovation Center for Marine Biomass Fiber Materials and Textiles, Laboratory of Fiber Materials and Modern Textile, The Growing Base for State Key Laboratory, Qingdao University, Qingdaom, 266071, PR China

[b] College of Chemical and Environmental Engineering, Shandong University of Science and Technology, Qingdao, PR China

ARTICLE INFO

Keywords:
Enzyme-mediated cascade reaction
Dual signal amplification
Thrombin
Homogeneous biosenor
Electrochemical detection

ABSTRACT

Enzyme-mediated cascade reaction is applied to amplify signal and decrease the background because enzyme can catalyze inactive substrates into active substrates to generate the signal. In this work, Au nanoparticles, as signal probe, are used to load DNA probe and ALP for dual signal amplification. Based on enzyme-mediated cascade reaction, a homogeneous biosensor is constructed for bioassay by employing thrombin as target molecule. When the target is present in the solution, ALP catalyzes the PPi into Pi and then reacts with molybdate in conjunction with Pi in the DNA backbone to produce redox precipitates on the surface of the reduced graphene oxide modified electrode with the help of magnetic separation. Compared with the conventional heterogeneous biosensor, the immobilization-free strategy, proposed in this homogeneous biosensor, improves the sensitivity because of its lower steric hindrance. As a result, this biosensor displayed a great sensitivity with a wide linear range from 1 fM to 10 nM and a detection limit of 0.26 fM, providing a promise and easy operating method for various proteins detection.

1. Introduction

The disease-related protein has received a great interest due to its important role in the fields of biological studies, clinical diagnostics and medical treatment. Therefore, developing a simple, sensitive, selective and cost effective strategy for protein detection has great value (De la Rica and Stevens, 2012; Gubala et al., 2012; Rodríguez-Lorenzo et al., 2012; Rusling, 2013; Zhu et al., 2013; Gao et al., 2014). Among them, biosensor is a kind of useful device for the disease-related protein detection. Biosensor is divided into different types according to different molecular recognition parts and signal conversion parts, including of enzyme biosensor, immunobiosensor, electrochemical biosensor and so on. At present, electrochemical biosensor acquires an ever-increasing attraction for targets detection owing to its obvious advantages of time-saving, simple operation, rapid response and compatibility with micromanufacturing technology (Yang et al., 2016; Cao et al., 2018). However, the conventional heterogeneous electrochemical biosensor usually immobilizes the signal probe on the electrode surface, which increases steric hindrance of the electrode surface and decreases the precision of the system. In order to overcome these drawbacks, a homogeneous electrochemical biosensor is constructed in this protocol, where an immobilization-free strategy is proposed. The hybridization between the target molecule and probe DNA, as well as the reaction, occurs in the solution instead of fixing on the surface of electrode. Therefore, the recognition efficiency is improved compared with conventional heterogeneous methods (Luo et al., 2008; Xuan et al., 2012; Liu et al., 2015; Zhang et al., 2018a,b).

Aptamers are single-stranded oligonucleotides which are isolated from random-sequence DNA pools through in vitro selection technique known as systematic evolution of ligands by exponential enrichment (SELEX) (Ellington and Szostak, 1990; Tuerk and Gold, 1990). Indeed, the separation process gives the aptamers ability to specifically bind to the targets ranging from metal ions (Kawakami et al., 2000), molecules (Zuo et al., 2007), proteins (Bang et al., 2013), even to cells (Wang et al., 2010). Due to these advantages of aptamers, they are thoroughly applied as recognition tools to bind the target molecule in the fabrication of a homogeneous electrochemical biosensor (Zhang et al., 2018a,b). In addition to being recognition tools, DNA can be used as the electric current source as well by applying the chemical energy stored in its bonds and the electric charge on the DNA phosphate backbone (Hu et al., 2017a,b). Since phosphate ion (Pi) can react with molybdate and generate the redox electric current, so the Pi in DNA backbone can

* Corresponding author.
E-mail address: xiajianfei@126.com (J. Xia).

https://doi.org/10.1016/j.bios.2019.111510
Received 13 June 2019; Accepted 12 July 2019
Available online 13 July 2019

react with molybdate to generate redox electric current (Xie et al., 2015; Hu et al., 2017a,b). Consequently, DNA was used as a signal resource for target detection in this protocol.

In order to get bigger signal current and lower detection limit, many kinds of signal amplification strategies have been proposed. Among them, the enzyme-mediated cascade signal amplification strategy has been widely employed, where the inactive substrates are catalyzed into active products by one type of enzyme (Qu et al., 2016; Shen et al., 2016). And then the active products could be used as a reactant for the next reaction, decreasing the background signal current compared with that of nonenzyme-catalyzed amplification (Hu et al., 2014; Qu et al., 2015; Kou et al., 2017). Xianyu et al. outlined an enzymatic cascade reaction for signal transduction and amplification by using horseradish peroxidase (HRP)-mediated aggregation of gold nanoparticles (Au NPs) (Xianyu et al., 2015). Jin et al. introduced a new concept to produce a phototriggered nanozyme through the ALP-based in situ biocatalytic process (Jin et al., 2015). Moreover, ALP is fully utilized in electrochemical biosensor to amplify signal due to its good properties in converting electroinactive species to electroactive species.

In this protocol, thrombin was chosen as the target, because of its important role in human life. Thrombin is a coagulation protein in the blood stream and relates to a multitude of diseases (Bichler et al., 1996; Holland et al., 2000). It is also capable of mediating neuroprotection against ischemia and environmental insults even with low concentrations (50 pM–100 nM) such as oxidative stress, hypoglycemia, hypoxia, and growth supplement deprivation (Wang et al., 2017). Based on DNA synergistic enzyme-mediated cascade reaction, a dual signal amplification homogeneous biosensor was constructed. I) DNA was not only used as aptamer to bind the target for improving the selectivity but also applied as the electric current source reacting with molybdate to generate redox current; II) In order to amplify the signal, Alkaline phosphatase (ALP) was utilized to catalyze the sodium pyrophosphate decahydrate ($Na_4P_2O_7{\cdot}10H_2O$, PPi) to generate the substrate, which reacted with the molybdate to generate the current. Au nanoparticles (Au NPs) were used as nanocarriers to load the DNA sequence and ALP forming signal probe. When the target was present, the thrombin binding aptamer (TBA) combined with the target and released the signal probe. With the aid of magnetic beads, the signal probe can be separated from the mixture for generating signal current. Therefore, the concentrations of thrombin could be detected with sensitivity and selectivity, which provided a promise for various proteins detection.

2. Experimental section

2.1. Chemicals and materials

Graphite powder (99.95%, 325 mesh) was purchased from Qingdao Jin Rilai Graphite Co., Ltd. (Qingdao, China). Carboxyl-modifed magnetic nanoparticles (MNPs) were obtained from BaseLine ChromTech Research Centre (Tianjin, China). 1-ethyl-(3-3′-dimethy-laminopropyl) carbodiimide (EDC), N-hydroxysuccini-mide (NHS), sodium molybdate and sodium pyrophosphate decahydrate ($Na_4P_2O_7{\cdot}10H_2O$, PPi) were ordered from Aladdin Reagent Co., Ltd. (Shanghai, China). Alkaline phosphatase (ALP) and thrombin were purchased from Sangon Biotechnology Co., Ltd. (Shanghai, China). The thrombin binding aptamer (TBA) and its complementary probe (CP) were synthesized and purified by Sangon Biotechnology Co., Ltd. (Shanghai, China) and the sequences were displayed in Table S1 (supporting information). The 50 mM Tris-HCl buffer solution (pH = 7.4), 10 mM phosphate buffer solution (PBS) (pH = 7.4, 100 mM NaCl) and 10 mM phosphate buffer solution (PBS) (pH = 7.0, 100 mM NaCl) were used as the buffer solutions. Other reagents were of analytical grade and used without further purification. All stock solutions were prepared with ultrapure water.

2.2. Apparatus

Electrochemical measurements were performed on the PARSTAT 4000 A electrochemical workstation (Princeton, America) applying a conventional three-electrode system. Among them, reduced graphene oxide modified glassy carbon electrode (GCE), Ag/AgCl electrode and platinum wire were used as working electrode, reference electrode and auxiliary electrode respectively. Transmission electron microscopy (TEM) characterization was carried out on a JEM-1200EX transmission electron microscope (JEOL, Japan). Scanning electron microscopy (SEM) characterization was carried out on a JSM-7001F scanning electron microscope (JEOL, Japan). The Zeta potential of nanoparticles was performed on the NanoBrook 90Plus Zeta (Brookhaven Instruments Corporation, America). UV-vis measurements were performed on Synergy HT multifunctional enzyme labeling instrument (Biotek, America). The water was purified by Milli-Q (Millipore, America).

2.3. Preparation of reduced graphene oxide modified GCE

Graphene oxide was synthesized according to a modified Hummer's method. The as-prepared graphene oxide was dissolved into PBS buffer (pH = 7.0, containing 100 mM NaCl) forming 2 mg/mL colloidal solution. Then the reduced graphene oxide was deposited onto the electrode via one-step way applying cyclic voltammetry method with the potential from -1.5 V to 0.5 V at the scan rate of 25 mV s^{-1}. In addition, 10 cycles were chosen as the optimal electrodeposition cycles, the reduced graphene oxide modified GCE was used as working electrode.

2.4. Preparation of TBA-modified magnetic nanoparticles

Firstly, 60 μL of carboxyl-modified MNPs were washed with PBS buffer (pH = 7.4, 100 mM NaCl) three times thoroughly and then MNPs were dispersed into 120 μL PBS buffer solution. After that, 500 μL of mixture containing 0.1 M EDC and 0.01M NHS was added into the solution and incubated at room temperature for 50 min to activate carboxyl groups of MNPs. Then the mixture was separated via magnetic separation and washed with PBS buffer three times and redispersed into 120 μL PBS buffer solution. Finally, 300 μL of TBA (1 μM) was introduced into the mixture and kept at 37 °C overnight. Subsequently, the MNPs-TBA conjugates were washed magnetically three times and redispersed into 120 μL PBS buffer solution and stored at 4 °C for further use.

2.5. Preparation of ALP and CP modified Au nanoparticles

Au NPs, as nanocarrier to load ALP and CP, were reduced by citrate sodium. In brief, 100 mL of 0.01% (w/v) $HAuCl_4$ solution was boiled under vigorous stirring condition, then 2.5 mL of 1% (w/v) trisodium citrate was added quickly. After reaction for 30 min, the solution turned deep red, indicating the formation of AuNPs. Subsequently, the colloids were left to stir and cool, then stored at 4 °C for further use.

Before modification, the thiolated CP (50 μM) was activated in 0.1 mM TCEP which was dissolved into 50 mM Tris-HCl (pH = 7.4) buffer at room temperature for 1 h. Afterwards, 50 μL of ALP (1.3 mg/mL) was introduced into 1 mL of as-prepared Au NPs and stirred at room temperature for 3 h gently. Then 20 μL of thiolated CP was added, and kept for 24 h, after that, 100 μL of NaCl (1M) was applied to “age” the DNA probe and incubated for another 24 h and the mixture was centrifuged for 15 min at 12000 rpm and washed with 10 mM PBS buffer (pH = 7.4, containing 100 mM NaCl) three times. Finally, the resulting ALP-Au NPs-CP were resuspended in PBS buffer and stored at 4 °C for further use.

2.6. Construction of the DNA synergistic enzyme-mediated cascade reaction homogeneous electrochemical sensor

To prepare the proposed sensor, 20 μL of MNPs-TBA was reacted with 50 μL of ALP-Au NPs-CP to form the double-strand structure at 37 °C for 2 h with the supernatant was discard, the conjugates were magnetically washed 3 times and redispersed into 20 μL PBS buffer. Afterwards, 50 μL of different concentration of thrombin was added to the solution to achieve proximity binding strand displacement. And the reaction was carried out at 37 °C for another 2 h. Subsequently, with the aid of magnetic separation, the mixture was separated and the supernatant was collected for further detection.

2.7. Electrochemical measurements

To achieve the target detection, 5 μL of mixture containing Na_2MoO_4 and PPi were dripped onto the surface of reduced graphene oxide modified electrode followed by the addition of 5 μL of supernatant and incubated at room temperature for 40 min. Then the electrode was measured in 0.5 M H_2SO_4.

3. Results and discussions

3.1. Principle of the assay

The principle of the DNA synergistic enzyme-mediated cascade reaction for homogeneous electrochemical bioassay is illustrated in Fig. 1. In this bioassay, the binding aptamer of thrombin (TBA) is fixed onto the surface of magnetic nanoparticles forming TBA modified magnetic nanoparticles (MNPs-TBA) as the recognition probe. Meanwhile, the Au NPs are combined with ALP and DNA sequence forming the signal probe (ALP-Au NPs-CP). The DNA sequence and the TBA are able to be complementary to each other forming a double strand. When the target is present, the TBA can combine with thrombin and the signal probe is released which is proportional to the concentration of target. With the aid of magnetic separation, the supernatant containing signal probe is collected for generating signal. In the chemical reaction of the substrates, I) DNA was not only used as aptamer to bind the target for improving the selectivity but also applied as the electric current source to provide Pi reacting with molybdate to generate redox current (Hu et al., 2017a,b); II) In order to amplify the signal, ALP was utilized to catalyze the PPi to generate Pi, which reacted with the molybdate in the solution generating molybdatephosphate on the surface of electrode (Qu et al., 2016; Shen et al., 2016). Then the redox molybdatephosphate can produce two pairs of redox peaks via the electrochemical detection in 0.5 M H_2SO_4 solution. Through measuring the signal current, the detection of target is accomplished.

3.2. Characterization of the nanoparticles, double-strand conjugate

In this protocol, the ALP and DNA were fixed onto Au NPs. The process was revealed by UV-vis and zeta potential. The UV-vis spectra of Au NPs, the Au-DNA and ALP-Au-DNA are shown in Fig. 2A. For the Au NPs, a strong adsorption peak is displayed at 520 nm. And the absorption peak of Au-DNA shifts from 520 nm to 524 nm due to the decoration of DNA on the Au nanoparticles. After binding ALP and DNA sequence, the characteristic adsorption peak of Au NPs shifts from 520 nm to 525 nm. The red shift of adsorption peak of the nanoparticles indicates the formation of the ALP-Au-DNA structure (Chen et al., 2014; Cao et al., 2018). Meanwhile, zeta potential was applied to characterize the modification process of biomolecules on the surface of Au NPs. As shown in Fig. 2B, the Au NPs, obtained via the reduction of $HAuCl_4$ by trisodium citrate, are negatively charged due to the carboxylate of trisodium citrate and peaks at -59.2 mV (curve a). After biomolecules modification, Au-DNA and ALP-Au-DNA peak at -46.8 mV (curve b) and -26.7 mV (curve c) respectively due to the combination between biomolecules and Au nanoparticles. These results indicate the accomplishment of the ALP-Au-DNA. Besides, the characterization of MNPs, MNPs-TBA and double-strand complex by TEM is illustrated in Fig. 2. For the bare MNPs, the spherical nanoparticles with a diameter of about 110 nm can be seen in Fig. 2C. After decoration of TBA, MNPs-TBA exhibits a light color and thin band at the edge of the nanoparticles (Fig. 2D), which reveals the accomplishment of MNPs-TBA. As shown in Fig. 2E, at the surface of MNPs, many Au nanoparticles can be observed due to the complementary of TBA and CP of the ALP-Au-CP. These results indicate the feasibility of the experiment.

3.3. Electrochemical characterization of the sensor

Electrochemical detection was employed to test the feasibility of the DNA synergistic enzyme-mediated cascade reaction homogeneous biosensor. The reaction between Pi and molybdate is exhibited in eq (1). Meanwhile, eq (2) and eq (3) reveal the electron transfer between different redox states of Mo in the precipitate:

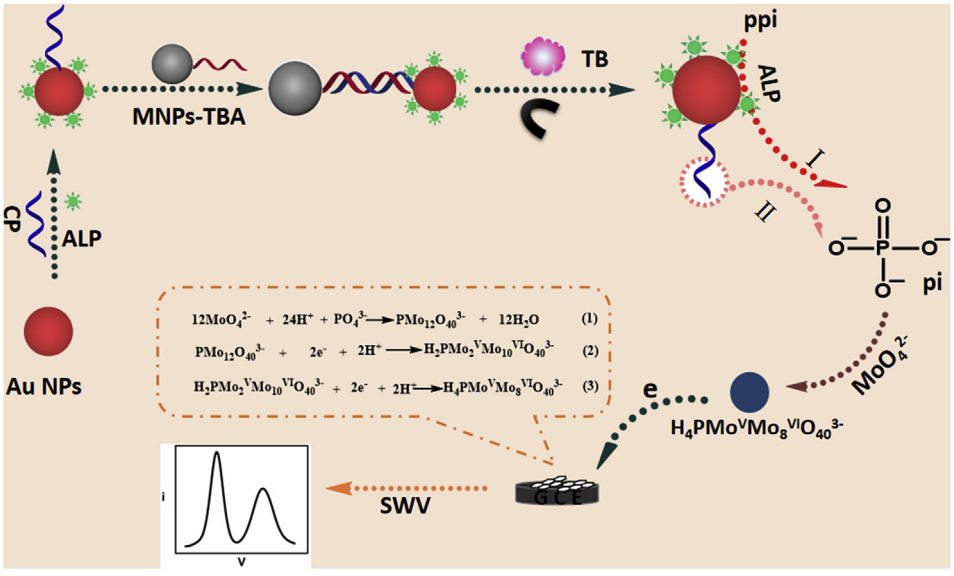

Fig. 1. Principle of the DNA synergistic enzyme-mediated cascade reaction for homogeneous electrochemical bioassay.

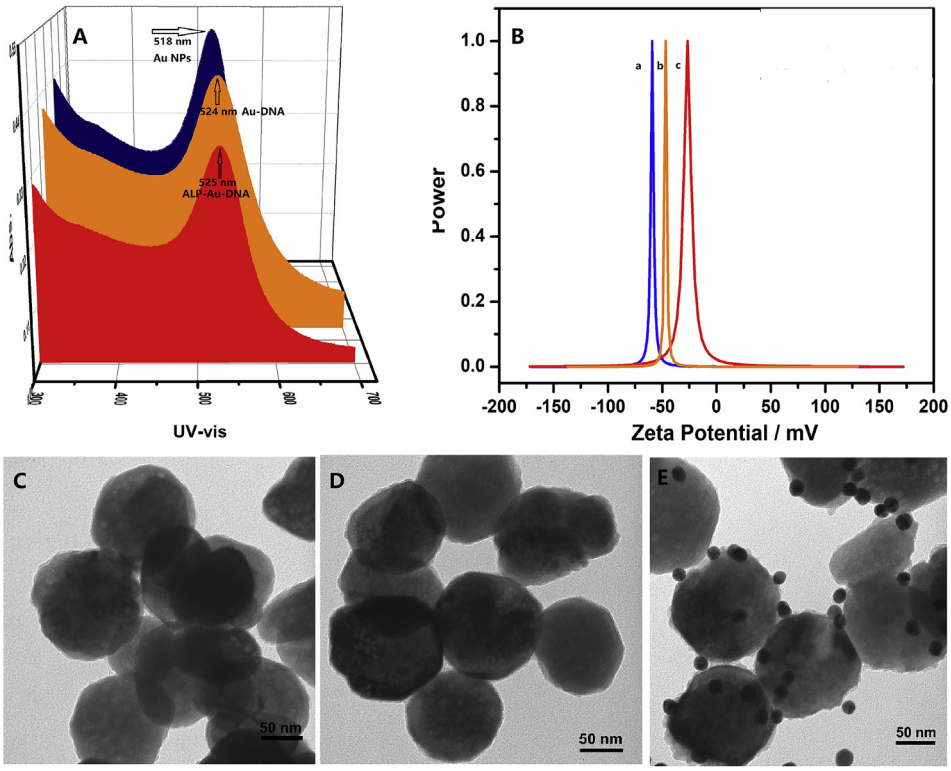

Fig. 2. UV-vis (A) and zeta potential (B) characterization of Au, Au-DNA and ALP-Au-DNA, TEM images of MNPs (C), MNPs-TBA (D), the double-strand structure (E).

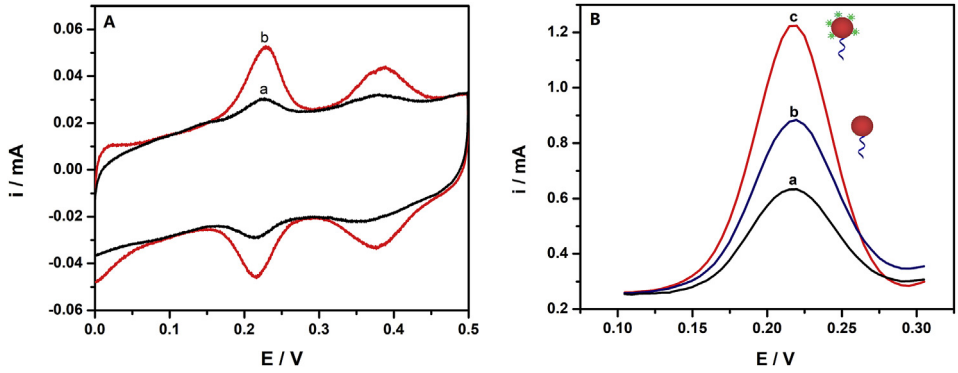

Fig. 3. (A) CV curves of the reduced graphene oxide modified GCE without thrombin (a), with thrombin (b) in 0.5 M H_2SO_4, the concentration of thrombin is 1×10^{-11} M. (B) SWV curves of the blank sample (a), Au-DNA signal probe (b) and ALP-Au-DNA signal probe (c).

As shown in Fig. 3A, when the target is present, there are two pairs of big peaks in the curve b, compared with the curve a, which is ascribed to the two different redox states of Mo (Hu et al., 2017a; Hu et al., 2017b).

In this protocol, ALP synergistic DNA reacted with molybdate to produce dual signal amplification and SWV methods were applied to compare the differences. As shown in Fig. 3B, DNA, as a source of signal, the Pi of its backbone can react with molybdate to generate a larger signal current when the thrombin is present (curve b) than blank sample (curve a). ALP, which is used for enzyme-mediated signal cascade amplification, can catalyze PPi to Pi and then reacts with molybdate in conjunction with Pi in the DNA backbone to generate signal current as the dual signal output (curve c). Under the dual signal amplification, a biggest signal current is achieved increasing the sensitivity of this experiment.

Reduced graphene oxide modified glassy carbon electrode (rGO/GCE) was used as working electrode to amplify the signal current. As shown in Fig. S1A (in the Supporting Information), at the surface of GCE, the reduced graphene oxide exhibits a wrinkle-like structure. The impedance spectra are shown in Fig. S1B. The Nyquist plot comprises a semicircular part at higher frequency range and a straight linear part at lower frequency range. The diameter of the semicircle equals electron transfer resistance (R_{et}). After modified reduced graphene oxide, the electrode exhibits a lower R_{et} than bare GCE because of the good electronic ability of reduced graphene oxide. In order to test the electrochemical properties of working electrode, the influence of scan rates on the electrochemical responses in $[Fe(CN)_6]^{3-/4-}$ solution was studied. As shown in Fig. S1C, the currents gradually increase with the increase of scan rates and a linear relationship is observed between the currents and the scan rates from 10 mV s^{-1} to 500 mV s^{-1}. The equations of linear regression are expressed as $i/\mu A = 0.278\ \upsilon/mV.s^{-1} + 46.081$ ($R = 0.990$) and $i/\mu A = -0.367\ \upsilon/mV.s^{-1} - 41.288$ ($R = 0.996$), indicating the rGO/GCE in $[Fe(CN)_6]^{3-/4-}$ solution is a adsorption-controlled process. Meanwhile, the electrochemical performance of rGO/GCE was investigated by CV methods (Fig. S1D). A large signal current (curve b) is produced in $[Fe(CN)_6]^{3-/4-}$ solution compared with bare electrode (curve a). The reason is that the reduced graphene oxide provides a large specific surface area, high conductivity and promotes

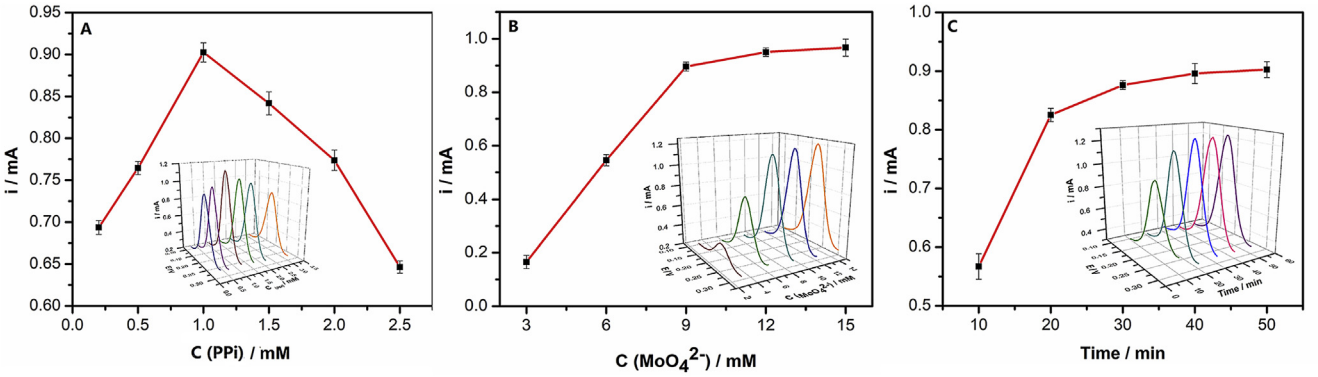

Fig. 4. The optimization of concentration of PPi (A, 0.2 mM, 0.5 mM, 1 mM, 1.5 mM, 2 mM, 2.5 mM), molybdate (B, 3 mM, 6 mM, 9 mM, 12 mM, 15 mM) and incubation time (C, 10min, 20min, 30min, 40min, 50min).

the electron and mass transfer. Above all, these results imply that the working electrode can amplify the signal for the target detection.

3.4. Analytical performance of the sensor

Several experimental parameters were optimized through the SWV in order to obtain good electrochemical performance. Firstly, the concentration of PPi is investigated ranging from 0.2 mM to 2.5 mM (Fig. 4A). Among them, from 0.2 mM to 1 mM, as the concentration increases, the signal current improves, which is ascribed to the fact that more PPi is catalyzed by ALP to Pi and then reacts with molybdate to form precipitates. When the concentration of PPi is increased from 1 mM to 3 mM, the signal current decreases a lot, due to PPi, with large molecule weight, stacked onto the surface of electrode and blocked the electron transfer. Then the concentration of molybdate is also optimized, as shown in Fig. 4B, as the molybdate concentration ranges from 3 mM to 15 mM, the signal current increases, which is attributed to the more precipitation of the phosphate and molybdate reactions, and gradually reaches the platform at a concentration of 12 mM. As the reaction time increases, the signal currents improve as well and do not change much after 40 min (Fig. 4C). Finally, the 1 mM of PPi, 12 mM of molybdate and a reaction time of 40 min were seleccted as the experimental conditions for further thrombin detection.

Under the optimal conditions, the quantitative determination of thrombin was carried out by SWV method. With the concentration of thrombin improves, the SWV peak current at around 0.21 V is increased (Fig. 5A), exhibits a good linear relationship between the peak current and the logarithm of thrombin concentration ranging from 1 fM to 10 nM. In addition, the equation of linear regression (Fig. 5B) is I/mA = 0.108 lgC/M + 2.021 (R = 0.998) with the detection limit of 0.26 fM (3σ rule).

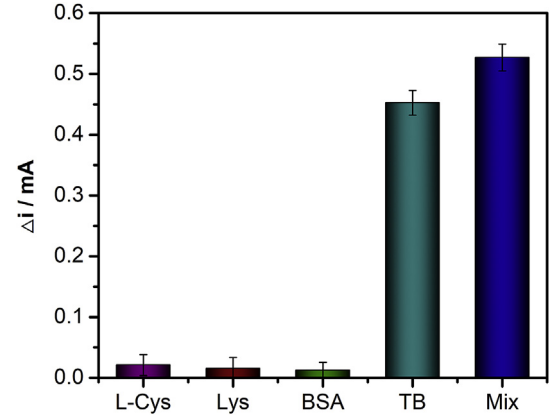

Fig. 6. Current responses of the aptasensor to L-Cys, Lys, BSA, thrombin and mixture of L-Cys, Lys, BSA and thrombin. The concentrations of BSA, Lys and L-Cystine were both 1×10^{-10} M, and the concentration of thrombin is 1×10^{-11} M. The error bar was calculated from three independent experiments. The current was referred to the difference value between the blank and actual value of targets ($\Delta i = i_{target}-i_{blank}$).

Furthermore, lysozyme (Lys), bovine serum albumin (BSA) and L-cysteine (L-Cys), are applied as interfering substances to investigate the specificity of the homogeneous biosensor by SWV method (Fig. 6). The electrochemical responses to these substances exhibit lower signal current while generate a higher current when the thrombin is present in the solution. The results indicate that the proposed dual signal amplification homogeneous biosensor is capable of detecting the thrombin

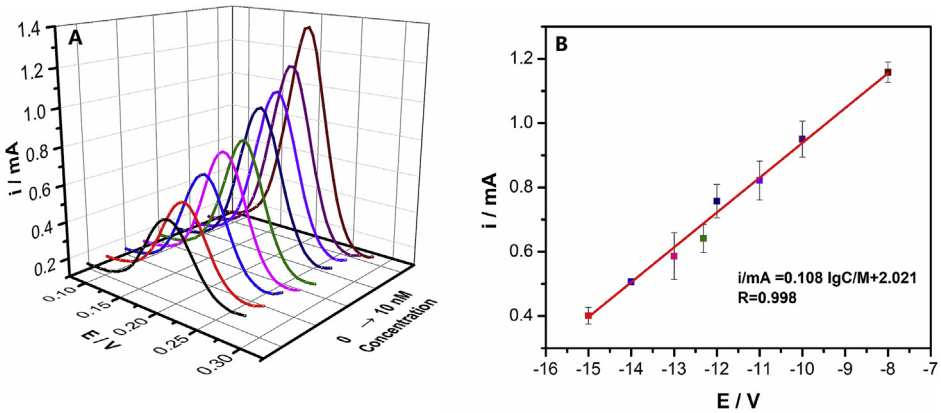

Fig. 5. SWV responses of the sensor to different concentrations of thrombin (1×10^{-15} M, 1×10^{-14} M, 1×10^{-13} M, 5×10^{-13} M, 1×10^{-12} M, 1×10^{-11} M, 1×10^{-10} M, 1×10^{-8} M) (A). The calibration curve for the peak current value versus the logarithm of thrombin concentration (B).

with high specificity.

In addition, the reproducibility and stability of the homogeneous biosensor have been researched. According to the standard biosensor fabrication and measurement process, five parallel measurements have been carried out for thrombin solution (the concentration is 1×10^{-11} M). A good reproducibility has been obtained with a low relative standard deviation (RSD < 5%). For stability investigation, the thrombin solution (the concentration is 1×10^{-11} M) has been detected six times by storing the homogeneous biosensor at 4 °C during 48 h. The low RSD (4.78) indicates that the proposed biosensor has a satisfactory stability.

3.5. Detection of thrombin in human serum samples

Furthermore, the several different concentrations of thrombin are detected by the proposed homogeneous biosensor in 100-fold diluted human serum (Table S2). The serum is obtained from healthy volunteers with the permission of local ethics committee. As shown in Table S2 (supporting information), the recovery rate of thrombin by electrochemical detection is 92.23%–97.85%. The results are acceptable and reveal a good reproducibility, indicating the applicability and reliability of the proposed strategy.

4. Conclusion

In summary, the proposed homogeneous biosensor generated a double amplified signal based on DNA synergistic enzyme-mediated cascade reaction, improving the sensitivity. In particular, DNA was used not only as a binding probe but also as a signal source, broadening its scope of amplification. Meanwhile, the structure formation and probe identification process occurred in homogeneous solution, which reduced the steric hindrance of the electrode surface and simplified the experiment. The dual signal amplification strategy improved the sensitivity and with the aid of reduced graphene oxide, this biosensor exhibited a good response toward thrombin ranging from 1 fM to 10 nM, holding a great promise to sensitively detect various targets such as DNA, metal ion, and protein. However, in this protocol, Au NPs was only used as a carrier to load DNA and ALP. For further improving the sensitivity and accuracy, it is an efficient way to design and prepare the multifunctional nanomaterials, which are used not only as nanocarrier to load biomolecule but also as signal amplifier or signal probe to generate multiple signals.

Declaration of competing interest

The authors declare that they have no known competing financial interests or personal relationships that could have appeared to influence the work reported in this paper.

Acknowledgments

We really appreciate the financial support from the National Natural Science Foundation of China (21645007, 21475071), the Taishan Scholar Program of Shandong Province (No.ts201511027) and the Natural Science Foundation of Shandong (ZR2016BM21).

Appendix A. Supplementary data

Supplementary data to this article can be found online at https://doi.org/10.1016/j.bios.2019.111510.

References

Bang, G.S., Cho, S., Lee, N., Lee, B.R., Kim, J.H., Kim, B.G., 2013. Biosens. Bioelectron. 39 (1), 44–50.
Bichler, J., Heit, J.A., Owen, W.G., 1996. Thromb. Res. 84 (4), 289–294.
Chen, X.J., Wang, Y.Z., Zhang, Y.Y., Chen, Z.H., Liu, Y., Li, Z.L., Li, J.H., 2014. Anal. Chem. 86, 4278–4286.
Cao, X.Y., Xu, J.Y., Xia, J.F., Zhang, F.F., Wang, Z.H., 2018. Sens. Actuators B Chem. 255, 2136–2142.
De la Rica, R., Stevens, M.M., 2012. Nat. Nanotechnol. 7 (12), 821–824.
Ellington, A.D., Szostak, J.W., 1990. Nature 346 (6287), 818–822.
Gao, Z.Q., Hou, L., Xu, M.D., Tang, D.P., 2014. Sci. Rep. 4, 3966.
Gubala, V., Harris, L.F., Ricco, A.J., Tan, M.X., Williams, D.E., 2012. Anal. Chem. 84 (2), 487–515.
Holland, C.A., Henry, A.T., Whinna, H.C., Church, F.C., 2000. FEBS Lett. 484, 87–91.
Hu, J., Jiang, Y.Z., Wu, L.L., Wu, Z., Bi, Y., Wong, G., Qiu, X., Chen, J., Pang, D.W., Zhang, Z.L., 2017a. Anal. Chem. 89 (24), 13105–13111.
Hu, L.S., Hu, S.Q., Guo, L.Y., Shen, C.C., Yang, M.H., Rasooly, A., 2017b. Anal. Chem. 89 (4), 2547–2552.
Hu, Y.W., Wang, F., Lu, C.H., Girsh, J., Golub, E., Willner, I., 2014. Chemistry 20 (49), 16203–16209.
Jin, L.Y., Dong, Y.M., Wu, X.M., Cao, G.X., Wang, G.L., 2015. Anal. Chem. 87 (20), 10429–10436.
Kawakami, J.J., Imanaka, H., Yokota, Y.K., Sugimoto, N.K., 2000. J. Inorg. Biochem. 82, 197–206.
Kou, B.B., Chai, Y.Q., Yuan, Y.L., Yuan, R., 2017. Anal. Chem. 89 (17), 9383–9387.
Liu, X., Li, W., Hou, T., Dong, S., Yu, G., Li, F., 2015. Anal. Chem. 87 (7), 4030–4036.
Luo, X.T., Lee, T.M.H., Hsing, M.I., 2008. Anal. Chem. 80 (19), 7341–7346.
Qu, F.L., Yang, M.H., Rasooly, A., 2016. Anal. Chem. 88 (21), 10559–10565.
Qu, R., Shen, L.L., Qu, A.T., Wang, R.L., An, Y.L., Shi, L.Q., 2015. ACS Appl. Mater. Interfaces 7 (30), 16694–16705.
Rodríguez-Lorenzo, L., de la Rica, R., Álvarez-Puebla, R.A., Liz-Marzán, L.M., Stevens, M.M., 2012. Nat. Mater. 11 (7), 604–607.
Rusling, J.F., 2013. Anal. Chem. 85 (11), 5304–5310.
Shen, C.C., Li, X.Z., Rasooly, A., Guo, L.Y., Zhang, K.N., Yang, M.H., 2016. Biosens. Bioelectron. 85, 220–225.
Tuerk, C., Gold, L., 1990. Science 249 (4968), 505–510.
Wang, L.L., Ma, R.N., Jiang, L.S., Jia, L.P., Jia, W.L., Wang, H.S., 2017. Biosens. Bioelectron. 92, 390–395.
Wang, Y., Li, Z.H., Hu, D.H., Lin, C.T., Li, J.H., Lin, Y.H., 2010. J. Am. Chem. Soc. 132 (27), 9274–9276.
Xianyu, Y.L., Chen, Y.P., Jiang, X.Y., 2015. Anal. Chem. 87 (21), 10688–10692.
Xie, S.B., Yuan, Y.L., Chai, Y.Q., Yuan, R., 2015. Anal. Chem. 87 (20), 10268–10274.
Xuan, F., Luo, X.T., Hsing, I.M., 2012. Anal. Chem. 84 (12), 5216–5220.
Yang, J.M., Dou, B.T., Yuan, R., Xiang, Y., 2016. Anal. Chem. 88 (16), 8218–8223.
Zhang, Y.X., Xia, J.F., Zhang, F.F., Wang, Z.H., Liu, Q.Y., 2018a. Biosens. Bioelectron. 120, 15–21.
Zhang, Y.X., Xia, J.F., Zhang, F.F., Wang, Z.H., Liu, Q.Y., 2018b. Sens. Actuators B Chem. 267, 412–418.
Zhu, C.Y., Zeng, Z.Y., Li, H., Li, F., Fan, C.H., Zhang, H., 2013. J. Am. Chem. Soc. 135 (16), 5998–6001.
Zuo, X.L., Song, S.P., Zhang, J.R., Pan, D., Wang, L.H., Fan, C.H., 2007. J. Am. Chem. Soc. 129 (5), 1042–1043.